Earthquakes and Structures, *Vol. 15, No. 5 (2018) 565-581*
DOI: https://doi.org/10.12989/eas.2018.15.5.565

Theoretically-based and practice-oriented formulations for the floor spectra evaluation

Stefania Degli Abbati[a], Serena Cattari[b] and Sergio Lagomarsino[*]

Department of Civil, Chemical and Environmental Engineering, University of Genoa, Via Montallegro 1, 16145, Genoa, Italy

(Received August 3, 2018, Revised September 19, 2018, Accepted September 20, 2018)

Abstract. This paper proposes a new analytical formulation for computing the seismic input at various levels of a structure in terms of floor response spectra. The approach, which neglects the dynamic interaction between primary structure and secondary element, is particularly useful for the seismic assessment of secondary and non-structural elements. The proposed formulation has a robust theoretical basis and it is based on few meaningful dynamic parameters of the main building. The method has been validated in the linear and nonlinear behavior of the main building through results coming from both experimental tests (available in literature) and parametric numerical analyses. The conditions, for which the Floor Spectrum Approach and its simplified assumptions are valid, have been derived in terms of specific interval ratios between the mass of the secondary element and the participant mass of the main structure. Finally, a practice-oriented formulation has been derived, which could be easily implementable also at code level.

Keywords: floor response spectra; nonlinear behavior; dynamic filtering effect; seismic analysis; secondary and non-structural elements

1. Introduction

The availability of a reliable formulation for floor response spectra is a critical issue for the seismic verification of different kinds of elements, such as: non-structural components in masonry, reinforced concrete or steel buildings; portions in masonry walls subjected to local mechanisms (out-of-plane response). These elements are very common both in new and in existing constructions and both in ordinary and monumental ones. They include parapets, gables, chimneys, mechanical appendages and equipment, curtain walls, partitions, battlements, among others (Fig. 1). Past earthquakes highlighted their significant vulnerability, which often results in severe damage or even collapse, with consequent economic loss or risk for fatal injury to the occupants.

In most cases, secondary elements turn out to be more vulnerable when located in the upper parts of the main structure, due to the dynamic amplification of the motion from the ground level to the base of the secondary element (Villaverde 1997). In §2 this physical phenomenon is explained with its potential evolution in both the linear and nonlinear fields of the main structural response, through the evidences of some experimental data available in literature.

Traditionally, it is possible to quantify the variation of the seismic input at different levels of a structure by following two different approaches (Villaverde 1997; Muscolino 1991; Chen and Soong 1988):

i) the *Combined Primary-Secondary System* (*P-S system*) approach, which explicitly studies the whole system formed by the main structure and the secondary element;
ii) the *Floor Response Spectrum Approach*, which is based on the hypothesis to neglect the dynamic interactions between the two systems and works then by sub-structuring. In this case, the problem is "just limited"

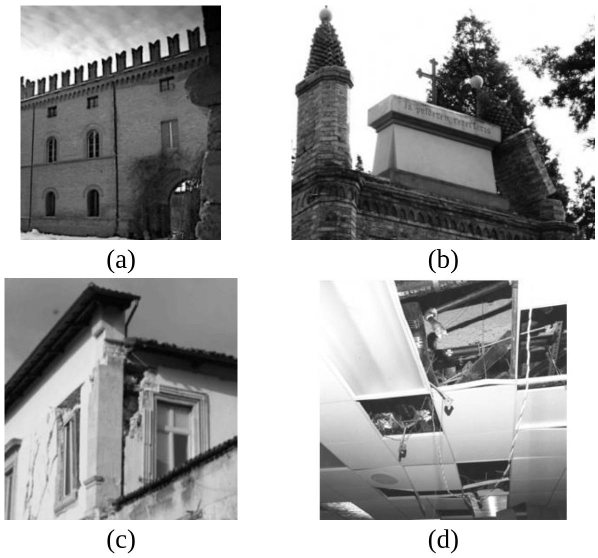

Fig. 1 Examples of: secondary elements like as (a) battlements and (b) parapets and spires; local mechanism in a masonry building (c); non-structural elements like as (d) false ceilings

∗Corresponding author, Full Professor
E-mail: sergio.lagomarsino@unige.it
[a]Ph.D.
E-mail: stefania.degliabbati@unige.it
[b]Assistant Professor
E-mail: serena.cattari@unige.it

ISSN: 2092-7614 (Print), 2092-7622 (Online)

to the correct definition of the floor spectrum.

The *Floor Response Spectrum Approach* (ii) allows obtaining the floor spectrum through a step-by-step integration of the filtered acceleration time history recorded at the floor where the secondary system is placed. However, this approach is barely attainable in engineering practice, since it requires lengthy numerical integrations. For this reason, some Authors soon after proposed several methods to generate floor response spectra directly from the ground response spectrum and by knowing the dynamic properties of the main structure as illustrated more in detail in §3. Starting from these proposals, various formulations have been derived and adopted in Standards as well.

Between the two aforementioned approaches, the formulation proposed in this paper (§4) belongs to the *Floor Response Spectrum Approach*. It aims to combine a robust theoretical basis and the capability to capture the main features of the actual phenomenon with a practice-oriented approach, useful in particular at engineering level. As documented in §5 and §6, the proposal has been validated through both experimental data available in literature and the results of numerical analyses performed *ad hoc*. In §7 its limits of application are discussed, with particular reference to neglect the dynamic interaction between the main and secondary systems. To this aim, a corrective factor is proposed that allows referring once again to the *Floor Response Spectrum Approach* even when the decoupling assumption is not completely legitimate. Finally, in §8 a code-oriented implementation of the proposed expression is presented.

2. Outcomes from laboratory and in-situ measurements

The seismic input on an element placed at a certain level of the building is a function of both the ground motion and the dynamic response of the primary structure, which may be affected by the evolution of the latter in the nonlinear range as well. Due to the complexity of the phenomenon, in-situ measurements on existing buildings or laboratory experimental tests are very useful: on one hand, to better understand its physics; on the other hand, to support the validation of analytical formulations.

In this section, the data acquired during a shake-table experimental campaign on a half-scale building are analyzed. As described below, such data are very useful to explore the role of filtering effect with the progressing of structural response from linear to nonlinear. The same data are then adopted in §5 to validate the proposed expression.

The campaign was developed by the *École Polytechnique Fédérale de Lausanne* (EPFL, Switzerland) at the TREES laboratory of the *European Centre for Training and Research in Earthquake Engineering* (EUCENTRE) in Pavia (Italy) (Beyer *et al*. 2015). The mock-up consisted in a half-scale four-story building, built with reinforced concrete (RC) and unreinforced masonry (URM) walls, as bearing system, connected by RC slabs (Fig. 2(a)). The input motion was the EW-component of the ground motion recorded at the Ulcinj-Hotel Albatross station during the April 15th, 1979, Montenegro earthquake.

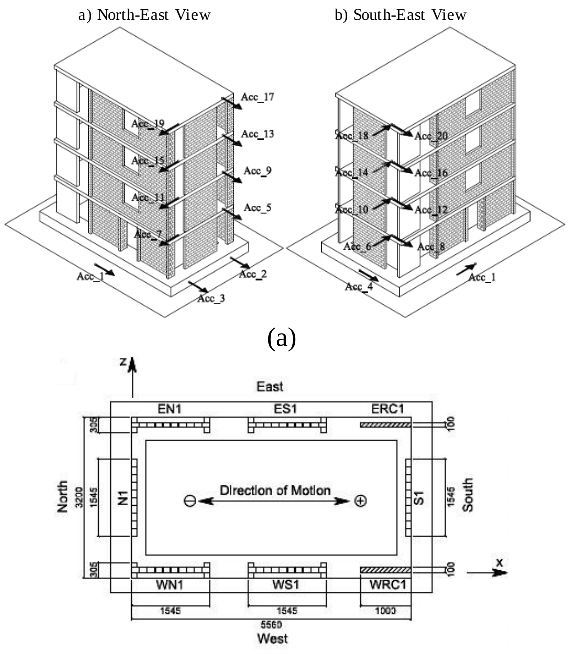

Fig. 2 (a) Sketch of the mock-up (total height equal to 6.2 m) and configuration of accelerometers; (b) Plan layout, dimensions in mm (Beyer *et al*. 2015)

The direction of motion was aligned with the longitudinal axis of the structure (Fig. 2(b)).

In the experimental campaign, the seismic input was scaled to match Peak Ground Acceleration (*PGA*) values ranging from 0.05 g to 0.9 g, up to inducing a significant damage state in the mock-up. From the test results (Beyer *et al*. 2015), it was possible to observe that the first three runs with a nominal *PGA* of the input (named PGA_{nom}) of 0.05-0.1-0.2 g induced only very limited damage to the structure; then, after runs 4 (PGA_{nom}=0.3 g) and 5 (PGA_{nom}=0.4 g), the first cracks appeared. During test 6 (PGA_{nom}=0.6 g), the damage to the structure was increased significantly. Then, test 7 (PGA_{nom}=0.4 g) was performed with a lower level of intensity than test 6 in order to simulate a possible aftershock, leading to a very little additional damage with maximum residual crack widths practically unaltered. Finally, tests 8 and 9 induced a severe damage to the structure.

Fig. 3(a) shows the floor response spectra generated from the acceleration time histories measured by the sensors at the fourth level and normalized to the value of PGA_{nom}. The figure compares the floor spectra of runs 1 and 6, when the mock-up was not damaged yet and significantly damaged, respectively. Furthermore, it illustrates the ground response spectrum obtained from the sensors placed on the shaking table (dashed line in Fig. 3(a)). It is worth noting that the actual movement of the shaking table is never exactly equal to the input record, due to the feedback of the equipment. Hence, the actual values of *PGA* at the shaking table are slightly different from the PGA_{nom}. For this reason, in Fig. 3(a) the shaking table response spectra normalized to PGA_{nom} do not start from 1.

Furthermore, Fig. 3 shows:

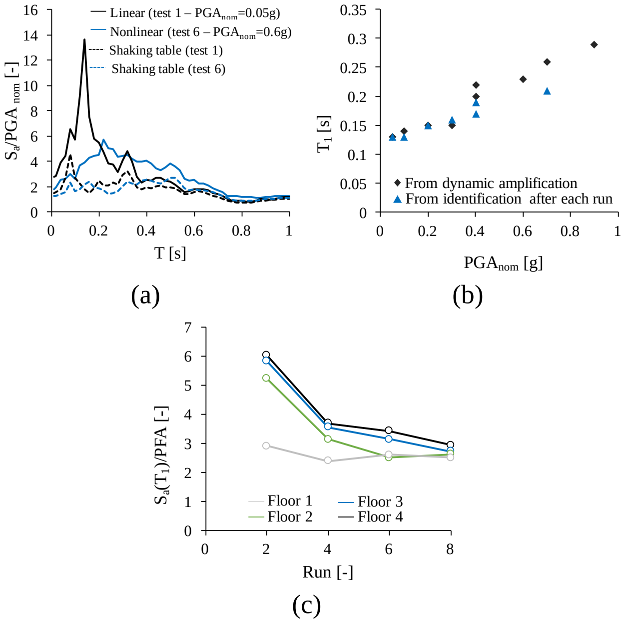

Fig. 3 (a) Comparison between floor (continuous lines) and ground (dashed line) response spectra obtained in the linear (test 1) and nonlinear field (test 6); (b) First period T_1 for different values of the PGA_{nom}; (c) Amplification factor ($S_a(T_1)/PFA$) with the consecutive runs and for each level

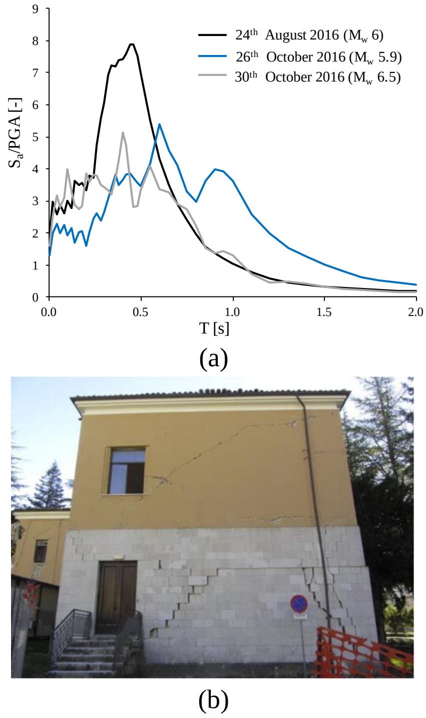

Fig. 4 (a) Floor spectra obtained from the recordings of sensors placed by OSS in the school of Visso (MC, Italy) after the consecutive shocks of the 2016 earthquake in the centre of Italy; (b) Example of damage level reached on the building after the last shock

- the evolution of the equivalent fundamental period (T_1) of the structure for increasing values of the PGA_{nom} (Fig. 3(b)): such values were determined respectively as the period with the largest dynamic amplification (rhombus indicator) or from the structural dynamic identification performed after each run test (triangle indicator, as illustrated in Beyer *et al*. 2015). These latter are generally shorter than the actual period obtained during the shaking;
- the variation of the amplification factor for consecutive runs (Fig. 3(c)). The amplification factor has been evaluated as the ratio between the spectral acceleration peak at the fundamental period of the structure ($S_a(T_1)$) and the Peak Floor Acceleration (*PFA*).

As it is possible to observe (Fig. 3(a)-(c)), as long as the response of the building is in the linear phase, significant amplifications can be observed both in terms *PFA* and spectral peak in correspondence of the fundamental period of the structure. Furthermore, the spectral accelerations are higher at the upper levels reaching the maximum amplification factor at the fourth story (Fig. 3(c)). Then, as the structure was increasingly damaged, the fundamental period of the structure lengthened (Fig. 3(a)-(b)), a significant reduction in the peak values of floor response spectra occurred (Fig. 3(a) and Fig. 3(c)) and, at the same time, the amplification peak tends to be smoother and wider (Fig. 3(a)).

The same effects have been testified by in-situ measurements on existing buildings. For example, in Italy, from the '90s, many structures (mostly ordinary buildings) are permanently monitored by the *Osservatorio Sismico delle Strutture* (OSS) of the Italian Department of Civil Protection (Dolce *et al*. 2017). This permanent monitoring program allowed to collect very precious data that support the evidence of a seismic amplification in the upper levels of actual buildings and of its evolution with the progressing of the main structure nonlinear response. For example, Fig. 4 shows the floor spectra obtained after the consecutive seismic shocks that hit the school of Visso (MC, Italy), significantly damaged by the 2016 earthquake and subjected to significant damage accumulation phenomena (Cattari and Sivori 2019, Reluis-Task 4.1 Workgroup 2017). Although these floor spectra have different shapes, because they come from different seismic events (while those obtained from experimental tests, in Fig. 3(a), are obtained by scaling the same record at the base), the same trends are evident (Fig. 4). In order to properly interpret the results, it has to be underlined that the building exhibited a significant damage after the 26th October 2016 second shake, while the occurred damage remained almost the same during the one of 30th October 2016.

3. State-of-the-art

3.1 Formulations in Standards

Many formulations for the floor spectra may be found in the Standards, usually in the framework of the seismic assessment or design of "non-structural elements". Only the Italian Technical Code, in particular in its related Instructions, proposes a different specific formulation for the verification of local mechanisms in existing masonry

Table 1 Comparison among different Standards formulations

Standard and adopted formulation			
CEN04 NTC08	$S_{a,Z} = a_g S \left[\dfrac{3\left(1+\frac{Z}{H}\right)}{1+\left(1-\frac{T}{T_1}\right)^2} - 0.5 \right]$	NZS 1170.5	$C_s(T_s) = C(0) \cdot C_{Hi} \cdot C_i(T)$
SIA 261	$S_{a,Z} = 2\gamma_f \dfrac{a_g}{g} S \dfrac{1}{q_s} \left[\dfrac{\left(1+\frac{Z}{H}\right)}{1+\left(1-\frac{T}{T_1}\right)^2} \right]$	ASCE/SEI 41-13	$S_{a,Z} = 0.4\, S_a \left(1 + 2\dfrac{Z}{H}\right)$
MIT09	$S_{d,Z} = S_d(T_1) \cdot \phi_1(Z) \cdot \Gamma_1 \dfrac{\left(\frac{T}{T_1}\right)^2}{\sqrt{\left(1-\frac{T}{T_1}\right)^2 + 0.02\frac{T}{T_1}}}$		

List of symbols (in alphabetic order):

a_g: Peak Ground Acceleration; C: site hazard coefficient; C_{Hi}: floor height coefficient, depending on the relative position of the secondary element; $C_i(T)$ secondary element's spectral shape factor defined as a tri-linear function; C_s: horizontal design coefficient; H: total height of the structure; q_s: q-factor of the non-structural element; S: soil amplification factor; S_a: response spectrum of ground acceleration; $S_{a,Z}$: acceleration floor spectrum; S_d: response spectrum of ground displacement; $S_{d,Z}$: displacement floor spectrum; T_1: first period of the structure; T: natural period of the secondary element; Z: level of the secondary element; γ_f: importance factor; Γ_1: coefficient of participation of the first mode; ϕ_1: modal shape of the first mode

structures. Table 1 compares the different expressions provided in the Standards herein considered, that are (in bracket the short acronym adopted is indicated): Eurocode 8 (CEN04 2004), Italian Building Technical Code (NTC08 2008) and related Instructions (MIT09 2009), New Zealand Code (NZS 1170.5 2006), American Standards (ASCE/SEI 41-13 2014), and Switzerland Standards (SIA 261 2003).

As it is possible to see from Table 1, in all Standards the floor spectrum is obtained starting from the seismic input at ground level (characterized either in terms of peak ground acceleration or spectral acceleration) and by accounting for the position of the non-structural element (mainly in terms of relative structural height *Z/H* at which the secondary element is placed); then, more or less simple analytical expressions are adopted. These latter involve the dynamic features of the main and secondary structures with a different level of accuracy, depending on the expression.

In fact, in some cases, that is the NZS 1170.5 and the ASCE/SEI 41-13, the base input is just amplified through coefficients which consider the level where the secondary element to be verified is placed or are dependent on the period of the secondary element. Conversely, in others, the main dynamic features of the structure are involved, too. However, it is interesting to point out that only the expression suggested in MIT09 involves the modal shape, the modal participation coefficient and the fundamental period, while in the other Standards (CEN04 and NTC08, SIA 261) only the structure fundamental period appears.

In order to highlight the differences and analogies among such formulations, the expressions of Table 1 have been applied to two case studies with different dynamic properties: a three-story masonry building and a nine-story RC one. In particular, the floor spectrum at the topmost story has been evaluated. Fig. 5 compares the results achieved. In particular, each color refers to a different expression, while the black dotted line indicates the value of the fundamental period of each building (T_1). The latter has been evaluated as $C_1H^{3/4}$(as proposed in NTC08) by assuming C_1 equal to 0.05 and 0.075 in the case of the masonry and the RC buildings, respectively. The total height H has been obtained (for both structures) assuming an inter-story equal to 3.2 m. The resulting values of the fundamental period are 0.27 s (for the masonry building) and 0.93 s (for the RC one). The input has been defined according to CEN04, assuming a soil of type A and then normalizing it to 1.

As evident from Fig. 5, the results are significantly scattered. The expressions that do not take into account the fundamental period of the structure obviously provide a constant floor spectrum amplification. CEN04 and SIA 261 define a floor spectrum with a peak in correspondence of the fundamental period T_1, but it depends only on the *PGA* and not on $S_a(T_1)$, thus resulting the same for the two case study buildings. Hence, they are not able to consider that for the RC building (and in general for flexible structures) the fundamental period intersects the descending branch of the ground response spectrum. MIT09 considers that the maximum amplification occurs in correspondence of the fundamental period of the structure; however, if compared with the other expressions, it determines higher values of the maximum amplification. Finally, despite the evidences from the experimental results discussed in §2, it is interesting to observe that no expression takes into account the effects of the nonlinear response of the main structure on the floor spectrum (Table 1).

3.2 Formulations in literature

A huge number of expressions are proposed in literature for the floor spectra definition.

The first methods date back to the '70s and were aimed to calculate the floor spectra for the assessment of equipment in power plants, hospitals and factories, due to the significant damage occurred after seismic events (Alaska 1964, Fernando 1971, Loma Prieta 1989). In that case, the main structure must not to be damaged, thus all these methods considered it as linear elastic. More recently, the floor spectra were introduced for the seismic verification of non-structural elements and local mechanisms in structures which can exhibit a marked

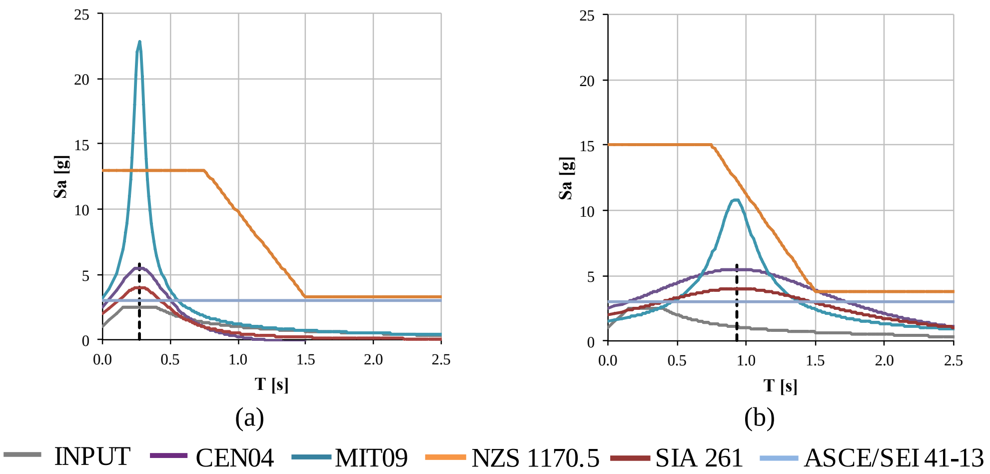

Fig. 5 Floor spectra at the topmost level for the three-story masonry building (a) and the nine-story RC building (b). The dotted line indicates the fundamental period of each building

nonlinear response as well, highlighting the relevance of including also such aspect.

Predictive equations in literature have adopted both analytical and numerical approaches and developed in a deterministic framework or, in few cases, in the probabilistic one (i.e., Singh 1975, Der Kiureghian *et al*. 1983, Lucchini *et al*. 2017). Hereafter, the attention is focused only on those belonging to a deterministic approach, that is the ambit of the new expression proposed in §4, and that have been proposed in the last decade.

Some of them have been mainly numerically calibrated through the execution of extensive parametric nonlinear dynamic analyses, like as the proposal of Menon and Magenes (2011a,b) or Sullivan *et al*. (2013), Calvi and Sullivan (2014). The first mainly investigated SDOF systems representative of masonry structures, while the second of RC structures varying in both cases the hysteretic properties of equivalent systems analyzed. Others, like as the formulations of Curti (2007) Lagomarsino (2015), have been derived from the original numerical-analytical dissertation by Singh (Singh 1975, Singh 1980, Burdisso and Singh 1987a,b) developing some more code-oriented proposals. In the latter ambit: Petrone *et al*. (2015) proposed a formulation explicitly derived for light non-structural components in European RC frame structures, that basically represents an extension of the one included in CEN04. The formulation was corroborated from the results of dynamic nonlinear analysis performed to a set of RC frame structures with different number of stories. Instead, Vukobratovic and Fajfar (2017), developed a code-oriented method, based on principles of structural dynamics and empirically determined values for the amplification factors in the resonance region. The latter represents a simplified version of the work presented in Vukobratovic and Fajfar (2015, 2016).

A synthetic overview of the various aspects of the physical phenomenon that such formulations are able to account for is illustrated below, by specifying the different level of detail adopted to describe each of them. In particular:

- the *features of the primary system* are considered respectively through: simply the fundamental period in Petrone *et al*. (2015); both the fundamental period and the equivalent damping in Calvi and Sullivan (2014) Menon and Magenes (2011); two or more modes in Curti (2007) Lagomarsino (2015), Vukobratovic and Fajfar (2017).
- The *features of the secondary system* are considered respectively through: simply the fundamental period in Menon and Magenes (2011) and by considering also its equivalent damping in all other proposal aforementioned.
- The *contribution of higher modes* is considered indirectly in Menon and Magenes (2011), Petrone *et al*. (2015), while explicitly in all other cases. In Petrone *et al*. (2015) the peaks in the higher modes are included considering the maximum envelope.
- The *seismic amplification* is considered through empirical or numerically calibrated multiplying factors in Calvi and Sullivan (2014), Petrone *et al*. (2015), Vukobratovic and Fajfar (2017) or as function of the fundamental or natural periods of the main structure as in Curti (2007), Magenes and Menon (2011) Lagomarsino (2015).
- The *nonlinearity of the primary system* is included only in few proposals (Calvi and Sullivan 2014, Menon and Magenes 2011, Vukobratovic and Fajfar 2017). In all these formulations, the effective period of the structure assumed as representative of the nonlinear response is one of the additional parameters which have to be defined. Then, further specific factors are introduced to: pass to the inelastic spectrum as in Calvi and Sullivan (2014), Vukobratovic and Fajfar (2017); account for the reduction of the peak and the widening bell in Menon and Magenes (2011).
- The *nonlinearity of the secondary system* is included only in few proposals and in implicit way by introducing the dependence on the equivalent damping representative of its response in nonlinear range (Curti 2007, Lagomarsino 2015, Calvi and Sullivan 2014, Vukobratovic and Fajfar 2017).

Differently from all the Standards examined in §3.1, it can be concluded that some literature formulations consider the systems nonlinearities and the contributions of higher modes, at least in a simplified way. Furthermore, they usually describe both the primary and the secondary systems with more details than in the Standards. Despite the higher level of detail, on the other hand, they often require the need to evaluate more parameters, sometimes empirically calibrated from the results of the performed analyses and this makes questionable their extrapolation to the use in any type of structures.

4. The proposed formulation

The proposed formulation allows obtaining the floor spectra just knowing the input response spectrum at the base of the structure and the dynamic parameters of all the relevant modes for the positions in the structure of interest. The analytical formulation is theoretically-based (§4.1) and conceived to be easily implementable in Standards; to this aim, all the involved parameters have a clear mechanical meaning (§4.2). Furthermore, the procedure takes into account the effects of the main building nonlinearities on the floor spectrum (§4.3) and the possibility to consider the contribution of different modes (§4.4).

4.1 Theoretical bases

The formulation proposed in this paper starts from the rigorous analytical/numerical dissertation originally presented by Singh (1975) and later developed in (Singh 1980, Burdisso and Singh 1987a,b). These studies were based on the assumptions that the ground motion is a zero mean Gaussian stationary random process and the main structure is linear elastic. Even if the first assumption is not actually verified for the seismic action, it has been shown that no substantial errors derive in the calculation of the floor spectra (Singh 1980). Burdisso and Singh's method allowed to determine the floor spectra only knowing the input at the base of the structure and the main dynamic features of the considered modes, properly selected as representative of the structural response.

Two characteristic points of the floor spectrum, in a given position of the main structure, are evaluated by a closed-form solution (Singh 1980, Burdisso and Singh 1987a, b) for the generic k^{th} of the N considered modes:

1. the Peak Floor Acceleration $PFA_{Z,k}$, which is the spectral ordinate in T=0 ($S_{aZ,k}(0)$);
2. the spectral ordinate in correspondence of the k^{th} natural period of the main structure $S_{aZ,k}(T_k)$.

In particular, the value of $PFA_{Z,k}$ is given by

$$\mathrm{PFA}_{Z,k} = S_a(T_k, \xi_k)|\Gamma_k \phi_k|\sqrt{1+4\xi_k^2} \tag{1}$$

where:

- the natural period T_k, the modal participation coefficient Γ_k and the modal shape $\phi_k(x,y,z)$ are the modal parameters of the primary structure;
- $S_a(T_k, \xi_k)$ is the spectrum at the base of the structure, calculated in correspondence of the natural period T_k.
- ξ_k is the viscous damping of the main structure.

Instead, the amplification peak due to the k^{th} mode is calculated by multiplying the $PFA_{Z,k}$ by an amplification factor (AMP_k) which substantially is a function of the viscous damping of the main structure ξ_k and of the secondary element ξ (Eq. (3))

$$\mathrm{S_{aZ,k}(T_k) = AMP_k\, PFA_{Z,k}} \tag{2}$$

where AMP_k is defined as

$$\mathrm{AMP_k} = \frac{\sqrt{\eta(\xi_k)^2 A_m + \frac{I_b}{S_e(T_k)^2}(1+4\xi^2 - A_m)}}{\eta(\xi_k)\sqrt{1+4\xi_k^2}\sqrt{1+4\xi^2}} \tag{3}$$

with A_m and I_b calculated as

$$\mathrm{A_m} = \frac{1+4(\xi^2+\xi_k^2+\xi\xi_k)+16\xi^2\xi_k^2}{4\xi_k(\xi+\xi_k)} \tag{4}$$

$$\frac{I_b}{S_a(T_k)^2} = \frac{1}{S_1(T_k)^2}\frac{\ln(T_D)-\ln(T_k)}{\ln(T_D)-\ln(T_B)} \tag{5}$$

being: T_B and T_D the characteristic period of the response spectrum at the ground floor (CEN04); $S_a(T_k)$ the elastic acceleration response spectrum at ground level, for 5% damping; $S_1(T_k)$ the one normalized to the PGA at ground level.

Elsewhere, for values of period different from T=0 and $T=T_k$, the floor spectrum was defined in each point, by the numerical solution of a system of equations, which cannot be solved in closed form. Therefore, a practice-oriented version of this formulation is proposed in §4.2, §4.3 and §4.4.

4.2 The proposed formulation: floor spectra for linear structures

The proposed formulation uses the closed-form solution by Singh (1980) and Burdisso and Singh (1987a, b) only to define the two characteristic points of the floor spectrum in T=0 and $T=T_k$, which can be calculated as

$$\mathrm{PFA}_{Z,k} = S_a(T_k)\eta(\xi_k)|\Gamma_k\phi_k|\sqrt{1+4\xi_k^2} \tag{6}$$

$$\mathrm{S_{aZ,k}(T_k) = AMP_k\, PFA_{Z,k}} = f_k\, f_s\, \mathrm{PFA_{Z,k}} \tag{7}$$

where:

- the $PFA_{Z,k}$ depends on the modal parameters of the main structure (T_k, Γ_k and $\phi_k(x,y,z)$) and its viscous damping ξ_k. Furthermore, it depends on the ground spectrum $S_a(T_k)$ calculated in correspondence of the structure's natural period T_k and properly reduced through the damping correction factor, unlike the original proposal by Singh (1980) and Burdisso and Singh (1987a,b) which prescribed instead $S_a(T_k, \xi_k)$ in a more general way. The damping correction factor of the main structure can be calculated for example as (CEN 2004)

$$\eta(\xi_k) = \sqrt{\frac{0.1}{0.05+\xi_k}} \geq 0.55 \tag{8}$$

with a reference value equal to 1 for ξ_k=0.05;

- the spectral ordinate in correspondence of the k^{th} natural period $S_{aZ,k}(T_k)$ is obtained as the $PFA_{Z,k}$

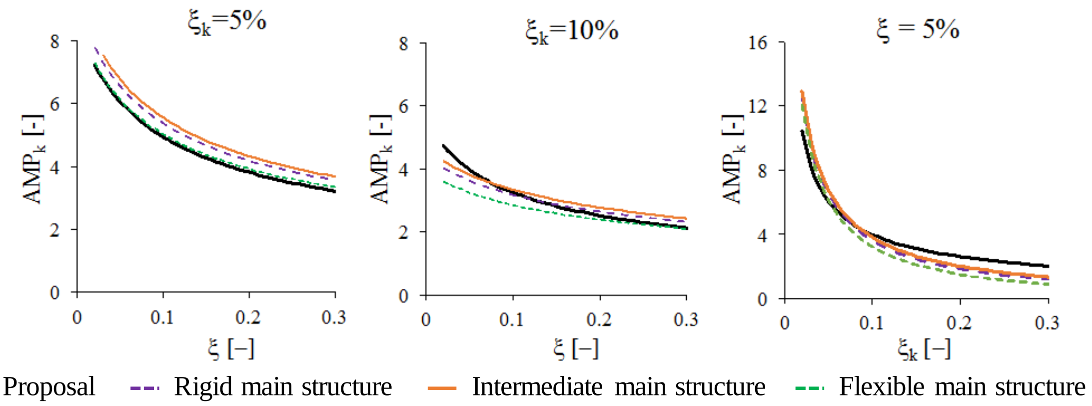

Fig. 6 Comparison of AMP_k according to the rigorous definition (colored lines) and the proposed simplified expressions (in black), by keeping constant respectively ξ_k and ξ

amplified through AMP_k. This latter directly derives from the theoretical one by Singh (1980) and Burdisso and Singh (1987a,b), but it has been organized in two contributions: f_k that depends only on the viscous damping of the main structure, and f_s that depends only on that of the secondary element. The expressions proposed to calculate these two contributions are

$$f_k = \xi_k^{-0.6} \tag{9}$$

$$f_s = \eta(\xi) = \sqrt{\frac{0.1}{0.05 + \xi}} \tag{10}$$

Fig. 6 shows the trend of AMP_k as obtained by the rigorous formulation (Eqs. (3)-(4)-(5), in colored lines) and the proposed expressions (black line) for f_k and f_s. A good fitting is highlighted. Referring to soil type A, three different situations have been considered for this comparison: 1) rigid structure (T_k=T_B); 2) intermediate structure (T_k=T_C); 3) flexible structure (T_k=1 s). In particular, Fig. 6 illustrates the results by alternatively keeping constant the viscous damping of the main structure ξ_k (ξ_k=5% and 10%) or the viscous damping of the secondary element.

Once defined the two characteristic points of the floor spectrum, elsewhere, the contribution to the floor spectrum due to the k^{th} mode is given by easy analytical expressions that pass through the above-mentioned values in T=0 and T=T_k and fit well the numerical solution of the rigorous formulation:

$$S_{aZ,k}(T,\xi) = \begin{cases} \dfrac{AMP_k\ PFA_{Z,k}}{1 + [AMP_k - 1]\left(1 - \frac{T}{T_k}\right)^{1.6}} & T \le T_k \\ \dfrac{AMP_k\ PFA_{Z,k}}{1 + [AMP_k - 1]\left(\frac{T}{T_k} - 1\right)^{1.2}} & T > T_k \end{cases} \tag{11}$$

Therefore, once properly selected all the interested modes and calculated the contribution of each one to the floor spectrum, the floor spectrum is obtained by using a modal combination rule. In this paper, a SRSS combination is proposed. The acceleration response spectrum $S_{a,Z}(T, \xi)$ of the filtered acceleration time history at the level Z of the building (floor spectrum at the point in the main structure identified by (x,y,z)), is then calculated as the SRSS combination of the contributions provided by the N modes considered as relevant for the response

$$S_{a,Z}(T,\xi) = \sqrt{\sum_{k=1}^{N} S_{aZ,k}^2(T,\xi)} \tag{12}$$
$$(\ge S_a(T)\eta(\xi) \quad \text{for} \quad T > T_1)$$

As it is indicated by the condition in brackets, for long periods the floor spectrum has to be taken always greater than the response spectrum of the ground motion because the structure is able to transfer in the upper levels the low-frequency contents of the ground motion itself (i.e., it behaves as "rigid" with respect to them).

Concerning the proper combination of modes, even herein the use of the SRSS modal combination rule is proposed. Other rules may be applied as well, for example when horizontal diaphragms are not rigid and natural periods are little different.

It is worth noting that, if the floor spectrum is evaluated from the response spectrum of ground motion acceleration $S_a(T_k)$ of an actual record, there is a strong sensitivity to the estimation of the period T_k, due to the presence of peaks and valleys in the response spectrum of ground motion. Hence, it could be suitable to evaluate the value of $S_a(T_k)$ as an average value in a proper range of periods around T_k (e.g., $T_k \pm 0.06$ s). In this way, the formulation allows obtaining floor spectra not only starting from a ground motion spectrum with a "smooth" shape (like the one of Standards), but also when the input consists of a real record, with a ground motion response spectrum having an irregular shape.

4.3 Effects of the nonlinear behavior of the main structure in the proposed formulation

The proposed formulation considers the nonlinear behavior of the building by assuming, as an approximation, a linear equivalent structure, by increasing both the period T_k and the damping ξ_k of all the modes for whom the nonlinearity occurs. It is worth noting that, for ordinary buildings, even when the contribution of higher modes is important, the nonlinearity involves only the fundamental modes in each direction, while higher modes may be

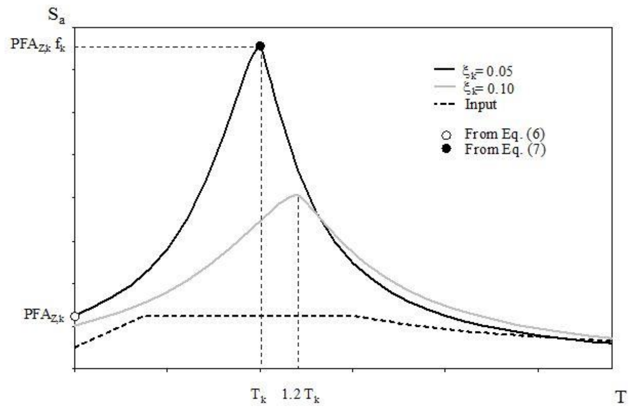

Fig. 7 Proposed analytical floor spectra in the linear and nonlinear phase of the structural response

considered elastic. In particular, for the former ones, in order to properly take into account the elongation of T_k due to nonlinearity, the period should be assumed as a mean value between the initial elastic period T_{ke} and a secant period corresponding to the ultimate displacement $\sqrt{\mu}T_{ke}$, where μ is the ductility demand on the equivalent SDOF representing the building:

$$\mathrm{T_k} = \mathrm{T_{ke}}\frac{1+\sqrt{\mu}}{2} \tag{13}$$

Coherently, the acceleration response spectrum should be calculated as:

$$S_a(T_k) = \frac{1}{(\sqrt{\mu}-1)T_{ke}}\int_{T_{ke}}^{\sqrt{\mu}T_{ke}} S_a(T)dT \tag{14}$$

Fig. 7 presents the proposed analytical floor spectra, calculated at the third level of a 4-storey building. A damping ξ_k equal to 5% (black line) and 10% (grey line) have been alternatively assumed and a period of the nonlinear building equal to $1.2T_{ke}$ (corresponding to a ductility demand for the main structure μ=2). The seismic input is the black dotted graph. From Fig. 7, it is possible to deduce the effects of the f_k parameter on the floor spectrum shape: with the nonlinear response of the main structure, the structural damping increases and, consequently, f_k decreases reducing the peak.

4.4 Criteria for the selection of the relevant modes

The formulation proposed is general and can be applied to any structure, once the modal analysis is performed. In particular, when the structure has flexible diaphragms (e.g., in the case of timber floors), many relevant modes should be considered, even close together in terms of corresponding periods and involving different parts of the structure, all with comparable mass participation coefficients. Hence, the floor spectrum in a certain point of the structure and for a given direction should be calculated considering those modes that significantly affect the *PFA* value. To this aim, it is sufficient to check the product $|\Gamma_k\phi_k(x,y,z)|$ and, according to this value, detect the higher modes that can be significant in the specific point under consideration. Moreover, in the case of flexible structures, higher modes can be relevant since the amplification on the first mode could be low being in the decreasing branch of the ground response spectrum.

Obviously, the proper selection of modes is a crucial step in the application of the proposed formulation and it is dependent on the kind of secondary element (or local mechanism) to be verified and for which the floor spectrum has to be calculated. For example, it is worth noting that if an accurate estimate of the floor spectrum in the low periods range is needed, the contributions of higher modes have to be considered. This is in particular true at lower levels in the building for the *PFA*. Conversely, if the secondary element to be verified is sensitive to the long periods, the contribution of the higher modes should be neglected, except in the case of local modes that are relevant for the specific point under consideration in the building. Once the modal analysis is performed and the relevant modes are selected, it is possible to easily calculate all the parameters to apply the proposed expression for the floor spectrum evaluation.

For multi-story buildings, regular in plan and with rigid or stiff horizontal diaphragms, it is often possible to neglect higher modes and consider only the contribution of the first mode in the direction of interest. In this case, the dynamic parameters may be evaluated in a simplified way and apply an easier engineering practice-oriented formulation, as proposed at §8.

5. Validation through experimental data

In order to validate the formulation proposed in §4, the results of the experimental campaign presented in §2 were adopted as reference. This section firstly summarizes all the data acquired from the experimental campaign and necessary to apply the new analytical expression for the floor spectra (§5.1); then, the results of the validation are presented (§5.2).

5.1 Description of the available experimental data

From the shaking tests illustrated in Beyer *et al*. (2015) it was possible to acquire: all data necessary to evaluate the analytical floor spectra through Eqs. (11)-(12); the experimental floor spectra generated from the acceleration time histories recorded by the sensors at each building level (located as in Fig. 2(a)).

Table 2 collects the available data for the 9 run tests: 1) PGA_{nom} of the run; 2) values of the periods T_1 and $T_{1,ID}$ used to estimate the level of nonlinear structural response; 3) corresponding ductility μ, evaluated from Eq. (13) by considering as reference elastic period $T_{1,run\,4}$=$T_{1,ID,run\,5}$=0.16 s, being the onset of damage in correspondence of those two runs (see Beyer *et al*. 2015); 4) value of the equivalent viscous damping of the main structure, derived from the peak of the recorded floor response spectra through Eq. (9); 5) values of the modal participation coefficient $\Gamma_{1,a}$ and $\Gamma_{1,b}$, calculated by assuming a modal shape ϕ normalized at the top, evaluated from the values of the *PFA* or from the peak $S_{aZ,1}(T_1)$, respectively. It has to be pointed out that the period T_1 is the one evaluated from the dynamic

Table 2 Summary of the main data used in the analytical floor spectra calculation

Run	PGA_{nom} [g]	T_1 [s]	$T_{1,ID}$ [s]	μ	ξ_1	$\Gamma_{1,a}$	$\Gamma_{1,b}$
1	0.05	0.13	0.13	0.4	0.05	1.331	1.329
2	0.1	0.14	0.13	0.6	0.05	1.317	1.328
3	0.2	0.14	0.13	0.6	0.05	1.355	1.345
4	0.3	0.16	0.15	1	0.08	1.231	1.299
5	0.4	0.20	0.16	2.2	0.12	1.139	1.340
6	0.6	0.23	0.17	3.5	0.12	1.167	1.288
7	0.4	0.22	0.17	3.1	0.09	1.130	1.304
8	0.7	0.26	0.19	5.0	0.15	1.236	1.298
9	0.9	0.29	0.21	6.9	0.16	1.258	1.203

amplification on the examined run, while the period $T_{1,ID}$ was obtained from the structural identification performed by the EPFL on the mock-up after each test. As expected, T_1 and $T_{1,ID}$ are almost equal during the first runs (when the structural response is linear), while they gradually increase when the structure is damaged, with $T_{1,ID}$ always lower than T_1. It is worth noting that the estimated maximum ductility demand, for Run 9, is compatible to values experimentally observed in Beyer *et al*. (2015).

Fig. 8 illustrates, for runs 2, 4 and 6, the comparison of the modal shapes respectively estimated from the *PFA* (Fig. 8(a)) and from the floor spectrum peak - $S_{aZ,1}(T_1)$ (Fig. 8(b)). As it is possible to observe, the modal shape ϕ obtained from the peak $S_{aZ,1}(T_1)$ exhibits the expected linear shape, apart the run 6 that shows the onset of a soft story behavior (really observed from shaking table tests). On the contrary, the ones evaluated from the *PFA* present higher values at the first two levels; this is due to the fact that *PFA* is influenced, in particular at the lower levels of the building, by the higher modes: therefore, the estimation of mode shapes from *PFA* is less accurate. These experimental modal shapes have been used to evaluate the Γ_1 and Γ_2 modal participation coefficients presented in Table 2.

The validation of the formulation proposed in §4 is based on the direct derivation of the equivalent viscous damping of the structure in correspondence of the peak of the recorded floor response spectra through Eq. (9), being known all other parameters in the formulation. Indeed, the obtained values (Table 2) are very reasonable: 1) before the occurrence of damage (run 1, 2 and 3) the value of the floor spectrum peak is obtained by assuming ξ_1=0.05 that is a widely-used reference value for mixed masonry-RC buildings; 2) after the occurrence of the damage, the equivalent viscous damping gradually increases up to a value of 0.16, which is also a typical value for damaged masonry buildings. In order to check the relation obtained between ductility and damping, these values (square indicators in Fig. 9) have been compared with the following analytical damping law (dashed line in Fig. 9), commonly assumed in literature for various building typologies (Calvi 1999; Blandon and Priestley 2005)

$$\xi = \xi_0 + \xi_H \left(1 - \frac{1}{\mu^{\beta}}\right) \tag{15}$$

In the examined case, the ξ_0 value is equal to $\xi_{1,run\,1,2,3}$=0.05, while for β and ξ_H a value equal to 0.8 and 0.14 has been

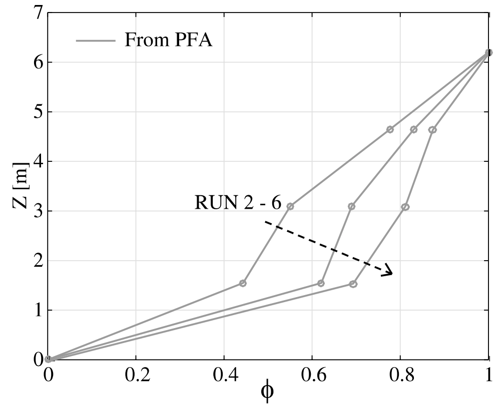

(a)

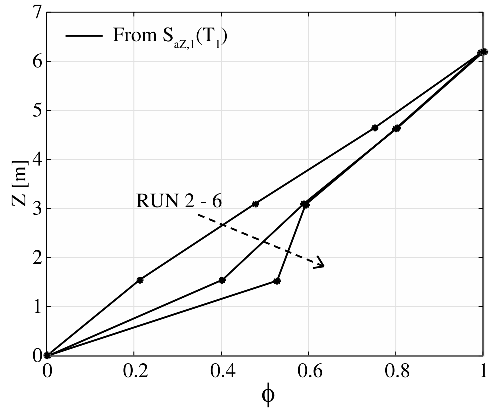

(b)

Fig. 8 Comparison of modal shapes for consecutive runs as obtained from: (a) *PFA*; (b) $S_{aZ,1}(T_1)$

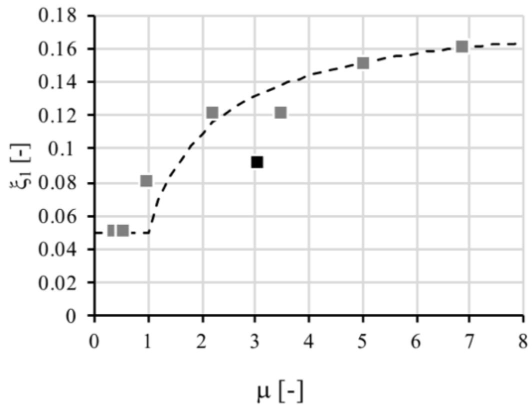

Fig. 9 Comparison between the adopted damping values (scattered indicators) and the analytical damping law expression (dashed black line)

assumed respectively, since these latter are values traditionally included in the range of those adopted for masonry structures (Cattari and Lagomarsino 2013a). Fig. 9 shows that the adopted analytical expression fits quite well the experimental data, except for the black indicator, which refers to run 7. However, it is worth noting that this latter was performed with a level of intensity lower than test run 6 and led only to a very little additional damage with maximum residual crack widths in practice unaltered.

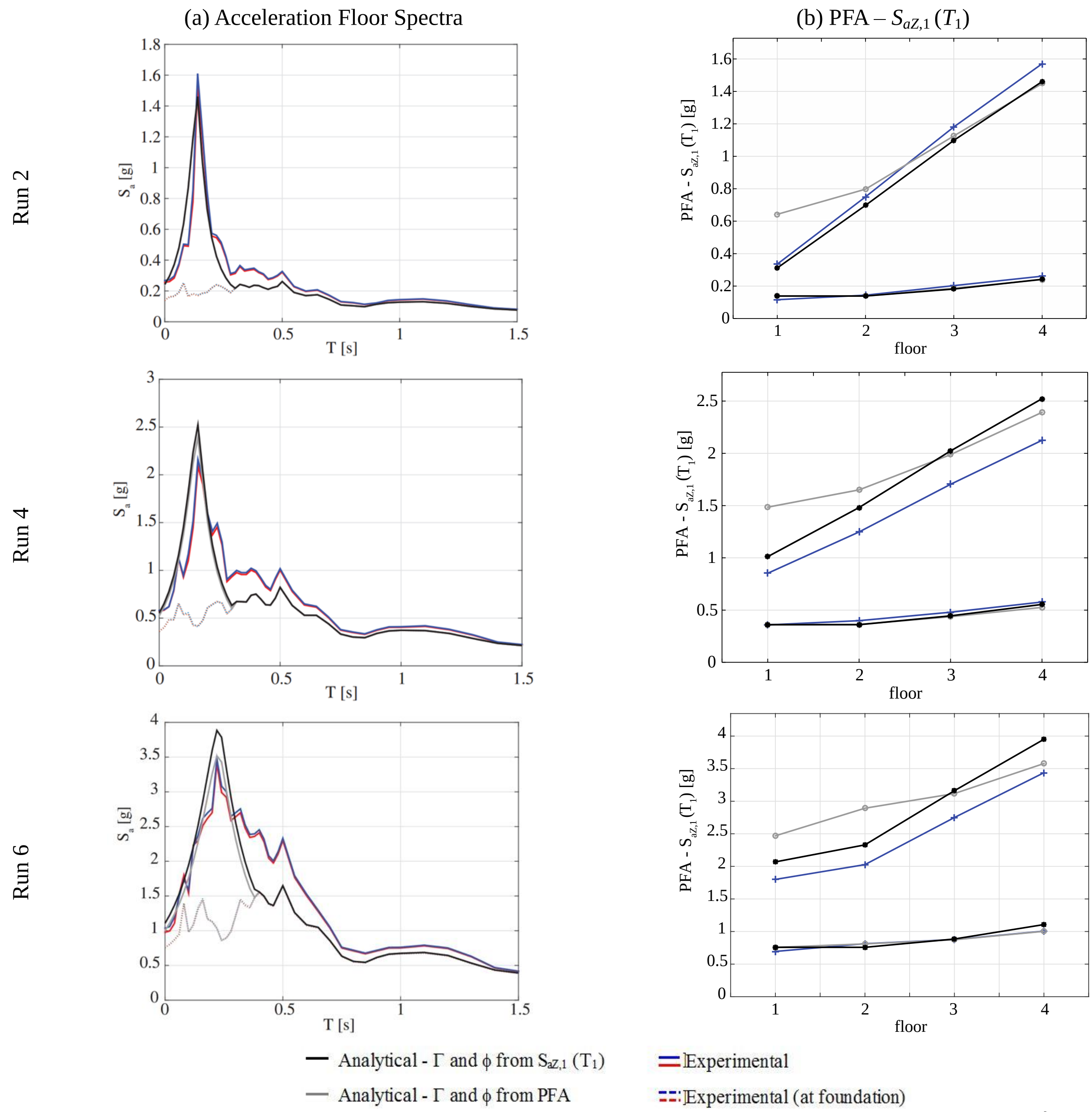

Fig. 10 Comparison for different runs in terms of experimental and analytical obtained: (a) floor spectra at the 4th level of the mock-up; (b) values of *PFA* and $S_{aZ,1}(T_1)$

Hence, the test unit was damaged, but with a less strong vibration: that means drift smaller than the one induced by test 6.

It is worth noting that the derivation of correct values of the equivalent viscous damping from the reverse application of the proposed formulation for floor spectra to experimental results on shaking table represents a significant validation because it means that Eqs. (7) to (9) are mechanically consistent.

5.2 Results of the experimental validation

In order to validate the proposed formulation in the linear and nonlinear phases of the structural response, for each run the experimental floor spectra have been compared with the analytical ones obtained through Eqs. (11)-(12). Fig. 10 presents the results of the experimental validation. In particular, the validation's results have been presented in Fig. 10 in terms of:

a. comparison between the experimental and analytical floor spectra: the experimental floor spectra recorded by the sensors at the fourth level (blue and red lines) are compared with the ones evaluated by applying the analytical proposed formulation, where Γ and ϕ have been respectively evaluated from the *PFA* (in grey) or from the $S_{aZ,1}(T_1)$ (in black); the corresponding response spectra at the shaking table are represented with the dotted lines (indeed, only one accelerometer was placed on the shaking table, which is rigid);

b. comparison between the experimental and analytical values of *PFA* (lower curves) and $S_{aZ,1}(T_1)$ (upper curves): the experimental values (marked in blue) are compared alternatively with the ones analytically obtained, with Γ and ϕ alternatively deduced again from the *PFA* (in grey) or from the $S_{aZ,1}(T_1)$ (in black).

From the comparison, it is possible to observe that:

i. by using the values of ϕ and Γ obtained from the *PFA*, the experimental values of *PFA* recorded at the different stories are better described. Instead, when ϕ and Γ are evaluated from the peaks, the best fitting between experimental and analytical data is in terms of maximum values of the response spectra;

ii. the proposed analytical formulation is able to simulate well the experimental data, especially when ϕ and Γ are obtained from the peak values of the response spectra. Despite this, the differences with those obtained from the peak $S_{aZ,1}(T_1)$ are quite moderate as well. It is worth noting that the expression proposed for f_1 (Eq. (9)) catches quite well the entity of the peak and its decrease when the structure behaves nonlinearly.

iii. with the progression of the structural response in the nonlinear range, in the floor spectra, secondary peaks come out for values of the period T higher than the fundamental one. This might be due to the contribution of local out-of-plane modes, characterized by lower frequency, which occurred because of the degradation of the connections between walls.

Table 3 Comparison among the results of the modal analyses

	Matlab (3-DOF)	Tremuri (3D model)
Modal shapes (First Mode)	0.381	0.397
	0.698	0.710
	1	1
First Period T_1	0.298 s	0.296 s

Table 4 Members of mass, stiffness and damping matrixes **M**, **K** and **C**

	1-1	1-2	1-3	2-1	2-2	2-3	3-1	3-2	3-3
M [kg] $\cdot 10^5$	2.460	0	0	0	2.097	0	0	0	1.433
K [N/m]$\cdot 10^9$	1.345	-0.676	0	-0.676	1.227	-0.532	0	-0.532	0.435
C [Ns/m] $\cdot 10^6$	1.932	-0.773	0	-0.773	1.739	-0.609	0	-0.609	0.726

Table 5 Considered values for T_1 and ξ_k, depending on the maximum ductility demand

	B1	**B2**	**B3**
μ	1	3.3	9
T_1[s]	0.298 s	0.42 s	0.596 s
ξ_1	5%	11.8%	15%

6. Numerical validation

In order to provide also a numerical validation of the proposed formulation, dynamic analyses have been performed on an elementary 3-DOF system by using Matlab. To this aim, the numerical floor spectra (as generated from the acceleration time histories filtered by the main building) have been compared with the ones obtained by applying the expressions proposed in §4. The building was alternatively considered linear and nonlinear through an equivalent elastic model with increased period and damping (§6.1). Different values of the damping of the secondary element (ξ=5% and ξ=3%) have been considered as well, in order to represent various types of secondary elements (Degli Abbati 2016). The dynamic analyses have been executed using as input 648 actual time histories selected to be compatible with the seismic action expected in L'Aquila at different return period. Such accelerograms have been selected within the framework of the RINTC project (Iervolino *et al.* 2018, RINTC Workgroup 2018).

6.1 Definition of the reference building model

The 3-DOF system was conceived in order to be representative of an existing masonry building (Cattari and Lagomarsino 2013b). For this reason, a three-dimensional detailed model was implemented with the Tremuri software (Lagomarsino *et al.* 2013), following the equivalent frame modelling strategy, where each wall is discretized as a frame of piers, spandrels and rigid nodes. The 3-DOF of the equivalent model are the horizontal translations of the three levels, taking into account also the spandrels flexibility that allows the nodes rotation.

In order to characterize the dynamic system, the mass matrix ***M*** and the stiffness matrix ***K*** have been evaluated. In particular, in the examined case, ***M*** is a diagonal matrix, where the components represent the sum of the nodal masses obtained in each level from the Tremuri model, while ***K*** has been numerically obtained from the detailed 3*D* model.

The correspondence between the complex 3D model and the equivalent 3-DOF system has been verified by performing a modal analysis. Table 3 compares the results, in terms of first period T_1 and modal shapes (normalized to the unity at the top).

The three natural periods deduced from the modal analysis were T_1=0.298 s, T_2=0.095 s and T_3=0.064 s. With these values and assuming a Rayleigh damping, the matrix ***C*** has been defined as proportional to the mass and stiffness matrixes ($\boldsymbol{C}=a_0\boldsymbol{M}+a_1\boldsymbol{K}$), in order to have a damping ξ equal to 5% for the modes 1 and 2. The coefficients a_0 and a_1 are equal to 1.5994 and 0.0011, respectively. Table 4 summarizes the values of the mass (**M**), stiffness (**K**) and damping (**C**) matrixes. Each column of Table 4 refers to the *i-j* component of each matrix (where *i*= matrix's row; *j*= matrix's column).

As briefly abovementioned, this building was analyzed under three different conditions of seismic response: linear behavior (B1); considering two different levels of maximum ductility demand (B2: μ=3.3; B3: μ=9). These values of maximum ductility correspond, through Eq. (13), to an average ductility of 2 and 4, respectively.

Table 5 illustrates for the three buildings the values of

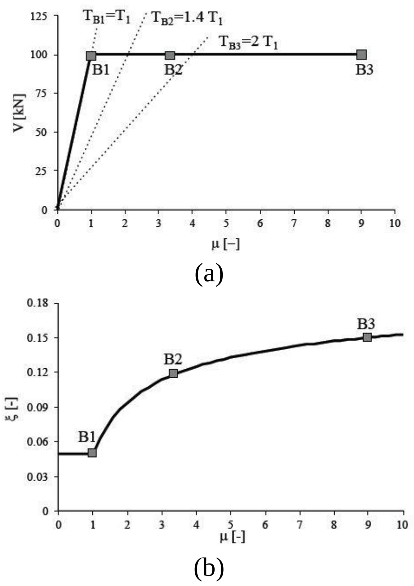

Fig. 11 Shear-ductility relation (a) and equivalent damping (b), according to Eqs.(13)-(15)

the maximum ductility μ, the fundamental period T_1 and the equivalent damping ξ_1.

For buildings B2 and B3 an equivalent elastic model, with stiffness matrix reduced by a constant factor, is considered (Fig. 11(a)). The equivalent damping ξ_k associated to the two different values of ductility is obtained from Eq. (15), assuming ξ_0=5%, ξ_H=20% and β=0.5 (Fig. 11(b)). These values are compatible with the ones proposed for masonry buildings (Cattari and Lagomarsino 2013a).

6.2 Results of the numerical validation

Fig. 12 illustrates the comparison between the numerical (dotted lines) and analytical (continuous lines) floor spectra, in terms of median value (in red), 16° percentile (in blue) and 84° percentile (in green). Also the ground response spectra is reported (the median value through the black continuous line; the 16° percentile and 84° percentile through the dotted grey lines).

All floor spectra are presented in the format of both

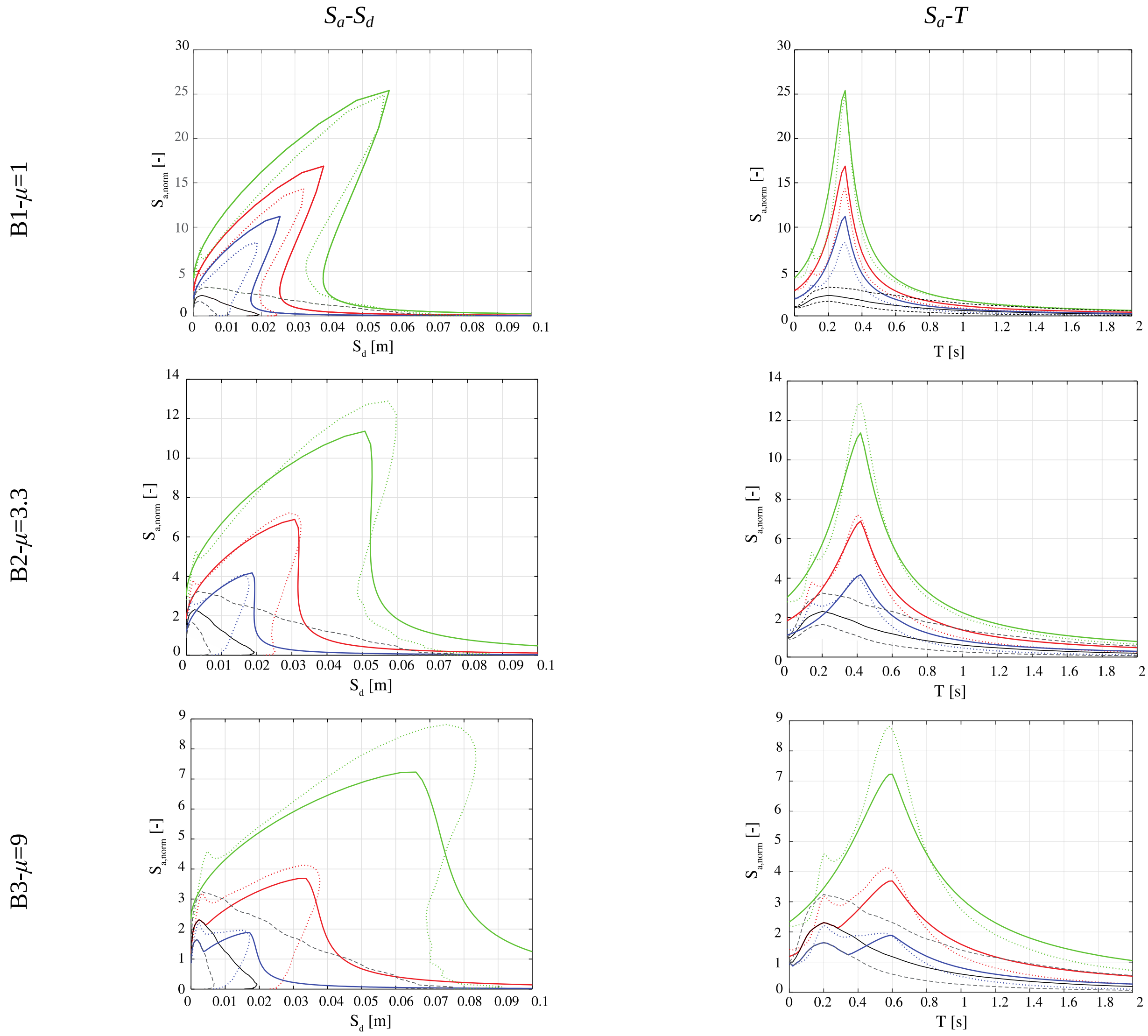

Fig. 12 Comparison between numerical (dotted lines) and analytical (continuous line) floor spectra (secondary element damping ξ=5%; building ductility: B1-μ=1; B2-μ=3.3 and B3-μ=9)

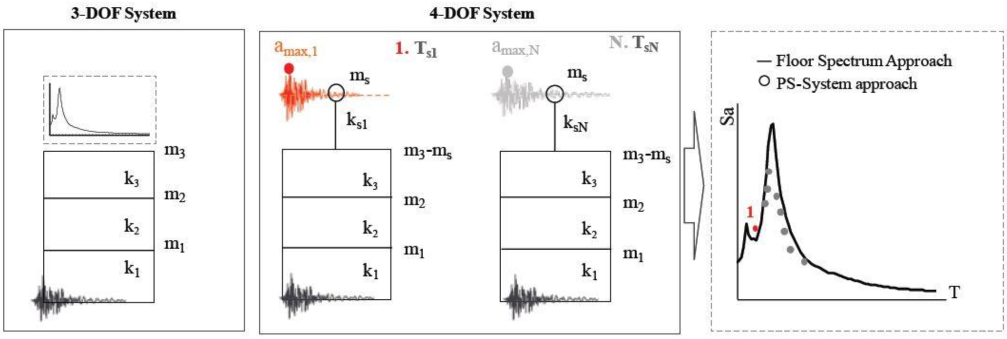

Fig. 13 Outline of the numerical methodology applied to obtain the floor spectrum by points

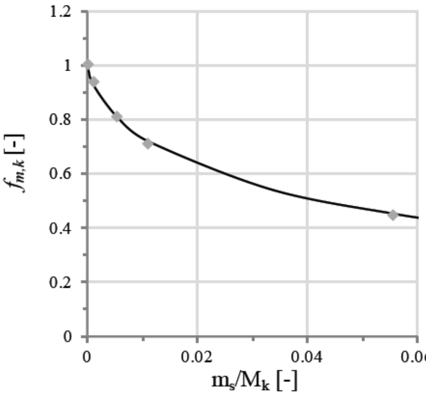

(a)

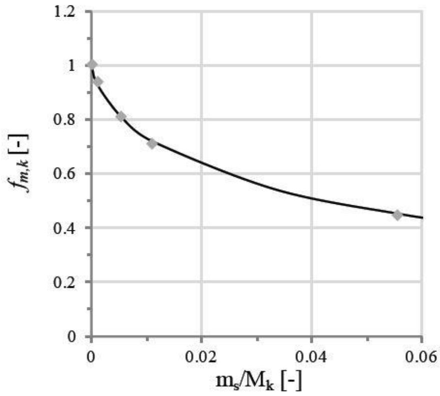

(b)

Fig. 14 (a) Comparison between the *Floor Response Spectrum Approach* and the *Combined P-S System approach*: results of the performed analyses; (b) Coefficient $f_{m,k}$ as a function of the m_s-M_k ratio, able to graduate properly the floor spectrum peak

acceleration-period and acceleration-displacement response spectra, for a damping equal to 5% of the secondary system. In the evaluation of the analytical floor spectra, for the sake of simplicity, only the contribution of the first mode is here considered. From Fig. 12, a general good agreement is observed although the analytical formulation slightly overestimates the floor spectra during the elastic response of the main structure, and slightly underestimates them when the primary system behaves in the nonlinear field (B3: μ=9).

7. Limits of application

As recalled in §1, the *Floor Spectrum Approach* is based on the assumption to neglect the dynamic interaction between primary structure and secondary element. In this section, the reliability of such assumption is verified by identifying the conditions when decoupling is possible.

To this aim, the acceleration floor spectra at the third level of the linear elastic 3-DOF system presented in §6.2 have been compared with the ones resulting by considering the whole system, that is the 4-DOF system where the further degree of freedom constitutes the secondary element (Fig. 13). As input for the dynamic analyses performed on such complete system, ten actual records from the 2009 L'Aquila earthquake have been used. In order to establish a complete coherence between the 3-DOF and 4-DOF systems, the secondary element mass m_s has been subtracted from the mass of the third level in the mass matrix $\boldsymbol{M}$. As far as the damping matrix $\boldsymbol{C}$ of the 4-DOF system concerns, a Caughy O' Kelly damping has been assumed to able to guarantee an initial damping equal to 5% on all the four modes (Eq. (16))

$$C = \sum_{j=0}^{N-1} \alpha_j (M^{-1}K)^j \tag{16}$$

The response spectrum to be compared with the analytical one has been then generated by points, varying the secondary element's stiffness k_s to obtain different values of the periods T_s (through the well-known equation $T_s = 2\pi\sqrt{\frac{m_s}{k_s}}$). Fig. 13 outlines the applied numerical methodology.

The analyses have been parametrically repeated by considering different values of the secondary element's mass (m_s) with respect to the global one of the building (M_{tot}), in order to consider different possible kinds of secondary elements (Fig. 14(a)). In particular, the m_s –M_{tot} ratio has been assumed respectively equal to: 0.05, 0.01, 0.005, 0.001.

Fig. 14(a) compares the floor spectrum at the third level of the 3-DOF system (grey line) with the ones evaluated point-by-point through the linear dynamic analyses performed on the 4-DOF system (marked with the scattered indicators and different colors varying the given m_s/M_{tot} ratio).

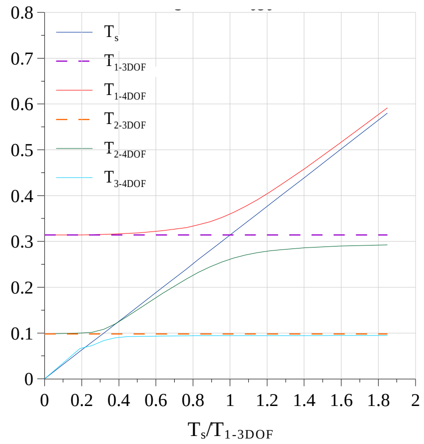

(a)

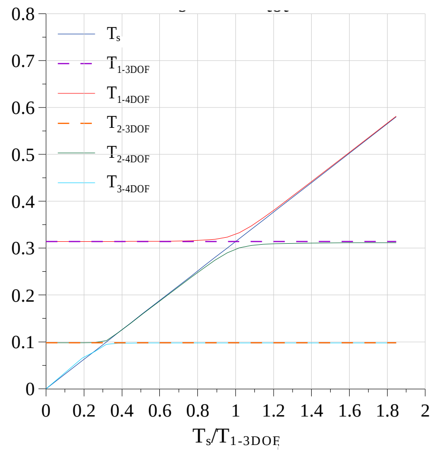

(b)

Fig. 15 Dependence of the periods T_s, $T_{1,4\text{-}DOF}$, $T_{2,4\text{-}DOF}$ e $T_{3,4\text{-}DOF}$ as a function of the ratio $T_s/T_{1,3\text{-}DOF}$, by varying the value of the secondary element's mass: (a) m_s=0.05M_{tot}, on the left; (b) m_s=0.005M_{tot}, on the right

The results of Fig. 14(a) highlight that: i) for secondary elements characterized by a negligible mass with respect to that of the main system, the floor spectrum obtained without considering the dynamic interaction with the main structure is correct; ii) otherwise, when the mass of the secondary element becomes significant, the *Floor Spectrum Approach* overestimates the actual spectral accelerations, especially in the range of periods close to the fundamental period of the primary system.

Fig. 15 allows interpreting these results more accurately. It shows, for two different masses of the secondary element, the period of the secondary element (T_s) and of the first, second and third periods of the 4-DOF system ($T_{1,4\text{-}DOF}$, $T_{2,4\text{-}DOF}$ e $T_{3,4\text{-}DOF}$) as a function of the ratio $T_s/T_{1,3\text{-}DOF}$ (being $T_{1,3\text{-}DOF}$ the first period of the 3-DOF system).

It is worth noting that, close to the unity (that is when T_s=$T_{1,3DOF}$), for decreasing values of the secondary element mass, the value of its period tends to become equal to the values of the first and second period of the 4-DOF system, that in turn tends to coincide with the first period of the 3-DOF system. This means that, when the secondary element has a negligible mass, the 4-DOF system is not influenced by the presence of this latter and it exactly behaves as the 3-DOF system. In other words, when the secondary element is characterized by a low mass, in correspondence to the peak of amplification, the whole system tends to have two periods almost equal: this justifies the presence of a significant amplification and the reliable use of a sub-structuring procedure. On the contrary, when the secondary element has a significant mass with respect to that of the primary structure, two equal periods never occur and the amplification tends to be reduced.

Starting from the peak acceleration values obtained from the numerical analyses performed on the 4-DOF system (Fig. 14(a)), a corrective factor $f_{m,k}$ to be applied to Eq. (7) has been calibrated in order to reduce the amplification on the k^{th} natural period as

$$f_k = f_{m,k} \cdot \xi_k^{-0.6} \tag{17}$$

The corrective factor $f_{m,k}$ is a function of the ratio m_s/M_k, where M_k is the participant mass on the k^{th} natural period. Fig. 14(b) shows the numerical values of $f_{m,k}$, which gradually decrease from 1 as the mass of the secondary element increases. A good fitting of these values is obtained by the following analytical formula

$$f_{m,k} = \left[1 + 9\left(\frac{m_s}{M_k}\right)^{0.7}\right]^{-1} \tag{18}$$

Even if an accurate numerical validation through a wide parametric analysis would be necessary, the proposed formula can be considered as a first proposal of a practice-oriented tool that allows referring to a *Floor Spectrum Approach*, even in case of the seismic assessment of secondary elements with non-negligible mass.

8. Engineering practice-oriented implementation for multi-story buildings with rigid diaphragms

As abovementioned, the formulation proposed in §4 is general and can be applied to any structure, once the modal analysis is performed and the relevant modes are selected. However, in the case of multi-story buildings, regular in plan and with stiff horizontal diaphragms, it is often possible to neglect higher modes and consider only the contribution of the first mode. In this ambit, an engineering practice-oriented implementation of the more general formulation is proposed below.

The floor spectra at the different levels of a multi-story building with rigid or stiff diaphragms and without significant torsional modes may be obtained by considering only the first mode of vibration in the direction of interest and evaluating all the dynamic parameters required by the formulation proposed in §4 in a simplified way. The modal shape can be defined as follows

$$\phi_1(Z) = \left(\frac{Z}{H}\right)^{\kappa} \tag{19}$$

where Z is the level of the secondary element, H is the total height of the building and κ is a proper coefficient. Usually κ=1 (inverse triangular modal shape) may be assumed for framed buildings, unless a soft storey is present at the base (κ<1); while κ>1 can be used in the case of slender shear

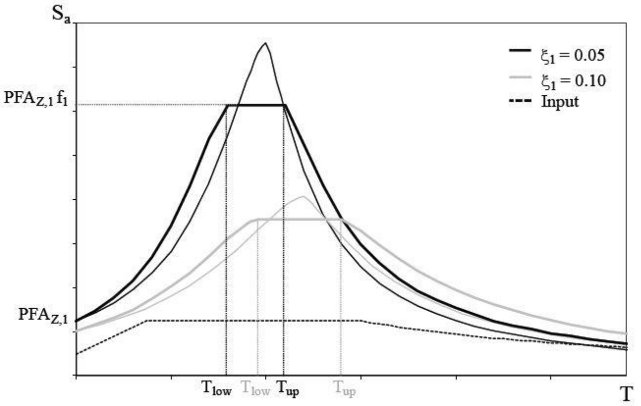

Fig. 16 Practice-oriented floor spectra in the linear and nonlinear phase of the structural response compared with the corresponding ones obtained through the theoretically-based expression

walls.

Regarding the modal participation coefficient, if it is possible to assume a linear modal shape and equal masses at the different floors, it is directly given by the number of stories N

$$\Gamma_1 = \frac{3N}{2N+1} \tag{20}$$

The fundamental period T_1 of the building in the direction of interest can be obtained through empirical relations, dependent on the total height or the number of stories, such as those proposed in Standards for the different structural materials (masonry, reinforced concrete, steel, timber) and types (frame, wall, etc.). This estimate is for sure affected by uncertainties, but it is worth noting that uncertainties cannot be avoided also by using a detailed numerical model (i.e., due to the influence of non-structural elements). For this reason, the simplified formulation here presented defines a plateau of maximum spectral amplification in the floor response spectrum, for a range of periods around the fundamental period which has been estimated, identified by the following lower and upper values: T_{low}=0.8T_1; T_{up}=1.1T_1. The spectral acceleration of this plateau is assumed a little bit lower than the sharp peak of the floor spectrum defined by Eq. (11), because it would be very conservative to use the peak for a wide range of periods. The proposed formulation for the factor f_1 (Eq. (9)) of amplification of the $PFA_{Z,1}$ is the following

$$f_1 = 1.1{\xi_1}^{-0.5} \tag{21}$$

which gives a reduction of the peak of less than 20% for ξ=0.05 and of 10% for ξ=0.15.

When the floor spectrum is derived with an input ground motion for which the main building is expected to behave nonlinearly with a maximum ductility demand μ, the reference value $T_{1,NL}$, for the period of the equivalent linear building to be used for the evaluation of $PFA_{Z,1}$ from (Eq. (6)), is given by

$$T_{1,NL}(\mu) = T_1 \frac{1+\sqrt{\mu}}{2} \tag{22}$$

The lower and upper periods of the plateau are then given by

$$T_{low} = T_1 \min\left[1; 0.4(1+\sqrt{\mu})\right] \tag{23}$$

$$T_{up} = 0.55(1+\sqrt{\mu})T_1 \tag{24}$$

Finally, the equivalent viscous damping ξ_1 can be assumed equal to 0.05, in the case a linear response of the main building is expected, or a larger value, as a function of the maximum ductility demand through Eq. (15).

In conclusion, for a multi-storey building regular in plan and with stiff horizontal diaphragms, the engineering practice-oriented formulation for the floor spectra, which considers only the contribution of the fundamental period in the direction of interest, can be expressed as follows

$$S_{aZ,1}(T,\xi) = \begin{cases} \dfrac{f_1\eta(\xi)PFA_{Z,1}}{1+[f_1\eta(\xi)-1]\left(1-\frac{T}{T_{low}}\right)^{1.6}} & T < T_{low} \\ f_1\eta(\xi)PFA_{Z,1} & T_{low} \le T \le T_{up} \\ \dfrac{f_1\eta(\xi)PFA_{Z,1}}{1+[f_1\eta(\xi)-1]\left(\frac{T}{T_{up}}-1\right)^{1.2}} & T > T_{up} \end{cases} \tag{25}$$

where T and ξ are the period and the damping of the secondary element.

Fig. 16 shows the floor spectra obtained through this practice-oriented expression compared with those obtained through the more general expression introduced in §4 (Fig. 7), considering the linear (black line) and nonlinear (grey line) behavior of the structural response. In the figure, the response spectrum of the input is drawn with the black dotted line.

9. Conclusions

This paper deals with the problem concerning the definition of reliable floor response spectra. This topic is relevant for the seismic verification of different kinds of elements, such as non-structural components in RC and steel structures or local mechanisms in masonry buildings. The critical discussion in §3 of the expressions already available highlighted that the methods in Standards provide results significantly scattered and sometimes overestimate the seismic demand on the secondary element; moreover, a significant drawback is that these methods neglect the effects of nonlinearities of the main structure. The formulations available in the literature are more rigorous but less practice-oriented, since they require the evaluation of many parameters, which are sometimes empirically calibrated making questionable their extrapolation to a huge variety of possible structures. The formulation proposed in the paper may be applied to any kind of structure and allows to include also the nonlinear behavior of the main building, although through a linear equivalent approach. The reliability of the formulation is demonstrated through experimental and numerical validations in both cases of linear and nonlinear behavior of the primary structure. It appears promising, being at the same time theoretically-based and straightforward in its application. In fact, it requires to know: the response spectrum at the ground floor; the damping of the main structure and of the secondary element; the modal parameters in terms of natural periods, deformed shape and modal participation coefficient of all the relevant modes. These latter can be easily determined from a modal analysis of the main structure, when available, or defined in a simplified way as presented in §8 in the engineering practice-oriented implementation of the proposed expression. Moreover, the applicability of the floor spectra approach in the case of secondary elements of non-negligible mass with respect to the one of the supporting building, has been verified by the comparison with results obtained by considering the dynamic interactions between primary system and secondary element. In this case, the dynamic interaction between the two systems determines a reduction of the amplification peak. Thus, a preliminary corrective factor is proposed as a function of the ratio between the mass of the secondary element and the participant mass of the main structure on the considered natural periods. It could be corroborated in future by a more extensive parametric analysis.

Acknowledgments

The results were achieved in the national research project ReLUIS-DPC 2014-2018 (www.reluis.it), supported by the Italian Civil Protection Agency. The Authors gratefully thank Prof. Katrin Beyer of EPFL (Lausanne, Switzerland), who provided the experimental data used in Section 5.2.

References

ASCE/SEI 41-13 (2014), Seismic Evaluation and Retrofit of Existing Buildings, American Society of Civil Engineers, Reston, VA, ISBN 978-0-7844-7791-5.

Beyer, K., Tondelli, M., Petry, S. and Peloso, S. (2015), “Dynamic testing of a four-storey building with reinforced concrete and unreinforced masonry walls: prediction, test results and data set”, *Bull Earthq. Eng*, **13**(10), 3015-3060.

Blandon, C.A. and Priestley, M.J.N. (2005), “Equivalent viscous damping equations for direct displacement based design”, *J. Earthq. Eng.*, **9**(sup2), 257-278.

Burdisso, R.A. and Singh M.P. (1987b), “Multiply supported secondary systems part II: seismic inputs”, *Earthq. Eng. Struct. Dyn.*, **15**, 73-90.

Burdisso, R.A. and Singh, M.P. (1987a), “Multiply supported secondary systems part I: response spectrum analysis”, *Earthq. Eng. Struct. Dyn.*, **15**, 53-72.

Calvi, G.M. (1999), “A displacement-based approach for vulnerability evaluation of classes of buildings”, *J. Earthq. Eng.*, **3**(3), 411-438.

Calvi, G.M. and Sullivan, T.J. (2014), “Estimating floor spectra in multiple degree of freedom systems”, *Earthq. Struct.*, **7**(1), 17-38.

Cattari, S. and Lagomarsino, S. (2013a), “Masonry structures”, *Developments in the Field of Displacement based Seismic Assessment*, Eds. T. Sullivan and G.M. Calvi, 151-200.

Cattari, S. and Lagomarsino, S. (2013b), “Seismic assessment of mixed masonry-reinforced concrete buildings by non-linear static analyses”, *Earthq. Struct.*, **4**(3), 241-264.

Cattari, S. and Sivori, D. (2017), “Lessons from the 2016 Central Italy earthquakes: the seismic behaviour of two masonry schools in Visso and Caldarola (Marche Region)”, *Bull. Earthq. Eng.* (submitted)

CEN (2004), Eurocode 8: Design of Structures for Earthquake Resistance-Part 1: General Rules, Seismic Actions and Rules for Buildings, European Code EN 1998-1, European Committee for Standardization, Brussels.

Chen, Y. and Soong, T.T. (1988), “State of art review seismic response of secondary systems”, *Eng. Struct.*, **10**, 218-228.

Curti, E. (2007), “Vulnerabilità sismica delle torri campanarie: modelli meccanici e macrosismici” Ph.D. Dissertation, University of Genoa, Genoa, Italy (in Italian).

Degli Abbati, S. (2016), “Seismic assessment of single-block rocking elements in masonry structures”, Ph.D. Dissertation, University of Genoa, Genoa (Italy).

Der Kiureghian, A., Sackman, J. and Nour-Omid, B. (1983), “Dynamic analysis of light equipment in structures: response to stochastic input”, *J. Eng. Mech.*, **109**(1), 90-110.

Dolce, M., Nicoletti, M., De Sortis, A., Marchesini, S., Spina, D. and Talanas, F. (2017), “Osservatorio sismico delle strutture: the Italian structural seismic monitoring network”, *Bull. Earthq. Eng.*, **15**, 621-641.

Grunthal, G. (1998), “European macroseismic scale”, *Conseil de l’Europe, Cahiers du Centre Europe´en de Ge´odynamique et de Se´ismologie*, Vol. 15, Luxembourg.

Iervolino, I., Spillatura, A. and Bazzurro, P. (2018), “Seismic reliability of code-conforming italian buildings”, *J. Earthq. Eng.*, DOI: 10.1080/13632469.2018.1540372.

Lagomarsino, S. (2015), “Seismic assessment of rocking masonry structures”, *Bull. Earthq. Eng.*, **13**(1), 97-128.

Lagomarsino, S., Penna, A., Galasco, A. and Cattari, S (2013), “TREMURI program: an equivalent frame model for the nonlinear seismic analysis of masonry buildings”, *Eng. Struct.*, **56**, 1787-1799.

Lucchini, A., Franchin, P. and Mollaioli, F. (2017), “Uniform hazard floor acceleration spectra for linear structures”, *Earthq. Eng. Struct. Dyn.*, **46**(7), 1121-1140.

Matlab® (2017), Theory Manual, Version R2017a.

Menon, A. and Magenes, G. (2011a), “Definition of seismic input for out-of-plane response of masonry walls: I. Parametric study”, *J. Earthq. Eng.*, **15(**2), 165-194.

Menon, A. and Magenes, G. (2011b), “Definition of seismic input for out-of-plane response of masonry walls: II. Formulation”, *J. Earthq. Eng.*, **15**(2), 195-213.

MIT (2009), Ministry of Infrastructures and Transportation, Circ. C.S.Ll. Pp. No. 617 2/2/2009, Istruzioni per l’applicazione delle nuove norme tecniche per le costruzioni di cui al Decreto Ministeriale 14 Gennaio 2008, G.U. S.O. n.27 of 26/2/2009, No. 47. (in Italian)

Muscolino, G. (1991), “Dinamica di sistemi strutturali composti da due sottostrutture”, Chapter contribution to the book *“Problemi Strutturali nell’Ingegneria Sismica”*, Dario Flaccovio Editore, 255-302. (in Italian)

NTC (2008), Decreto Ministeriale 14/1/2008. Norme tecniche per le costruzioni, Ministry of Infrastructures and Transportations, G.U. S.O. n.30 on 4/2/2008. (in Italian)

NZS 1170.5 (2006), Assessment and Improvement of the Structural Performance of Buildings in Earthquake, Recommendations of a NZSEE Study Group, New Zealand Society for Earthquake Engineering, Wellington, New Zealand.

Petrone, C., Magliulo, G. and Manfredi, G. (2015), “Seismic demand on light acceleration-sensitive nonstructural components in European reinforced concrete buildings”, *Earthq. Eng. Struct. Dyn.*, **44**, 1203-1217.

Reluis-Task 4.1 Workgroup (2017), S. Cattari, S. Degli Abbati, D. Ottonelli, D. Sivori, E. Spacone, G. Camata, C. Marano, F. Da

Porto, F. Lorenzoni, A. Calabria, A. Penna, F. Graziotti, R. Ceravolo, E. Matta, G. Miraglia, D. Spina, N. Fiorini, "Report di sintesi sulle attività svolte sugli edifici monitorati dall'Osservatorio Sismico delle Strutture", ReLUIS report, Rete dei Laboratori Universitari di Ingegneria Sismica, Naples. (in Italian)

RINTC Workgroup (2018), "Results of the 2015-2017 implicit seismic risk of code-conforming structures in Italy (RINTC) project", ReLUIS Report, Rete dei Laboratori Universitari di Ingegneria Sismica, Naples. Available at http://www.reluis.it/.

SIA 261 2003 (2003), Actions on Structures, Swiss Norm, Swiss Society of Engineers and Architects, Zurich.

Singh, M.P. (1975), "Generation of seismic floor spectra", *J. Eng. Mech. Div.*, ASCE, **101**(EM5), 593-607.

Singh, M.P. (1980), "Seismic design input for secondary systems", *J. Struct. Div.*, ASCE, **106**(ST2), 505-517.

Sullivan, T.J., Calvi, P.M. and Nascimbene, R. (2013), "Towards improved floor spectra estimates for seismic design", *Earthq. Struct.*, **4**(1), 109-132.

Villaverde, R. (1997), "Seismic design of secondary structures: state of the art", *J. Struct. Eng.*, ASCE, **123**(8), 1011-1019.

Vukobratovic, V. and Fajfar, P. (2015), "A method for the direct determination of approximate floor response spectra for SDOF inelastic structures", *Bull. Earthq. Eng.*, **13**(5), 1405-1424.

Vukobratovic, V. and Fajfar, P. (2016), "A method for the direct estimation of floor acceleration spectra for elastic and inelastic MDOF structures", *Bull. Earthq. Struct. Dyn.*, **45**(15), 2495-2511.

Vukobratovic, V. and Fajfar, P. (2017), "Code-oriented floor acceleration spectra for building structures", *Bull. Earthq. Eng.*, **15**(7), 3013-3026.

AT